Infrared Spectroscopic Study on Photolysis of Ethyl Iodide in Solid Parahydrogen: Perdeuterated Iodide System†

Norihito Sogoshi,‡ Tomonari Wakabayashi,‡ Takamasa Momose,*,‡ and Tadamasa Shida§

Division of Chemistry, Graduate School of Science, Kyoto University, Kyoto 606-8502, Japan, and Kanagawa Institute of Technology, 1030 Shimo-Ogino, Atsugi 243-0292, Japan

Received: October 31, 2000

Perdeuterated ethyl iodide in solid parahydrogen is photolyzed at 4.4 K to find the formation of all deuterated ethylene, ethane, and ethyl radical and deuterium iodide. The temporal change in the intensity of the vibrational spectra upon UV irradiation reveals that the initial ethyl iodide exists in both monomeric and dimeric units. The monomeric unit is subjected to the following competitive reactions: $C_2D_5I + h\nu \rightarrow \bullet C_2D_5 + \bullet I$ and $C_2D_5I + h\nu \rightarrow CD_2{=}CD_2 + DI$. The ethylene produced thereby is loosely complexed with the counterpart DI. The dimeric unit undergoes the following one-photonic parallel reactions I and II: (I) $(C_2D_5I)_2 + h\nu \rightarrow 2\bullet C_2D_5 + I_2$ to be followed by a gradual disproportionation, $2\bullet C_2D_5 \rightarrow CD_2{=}CD_2 + C_2D_6$, which proceeds by quantum tunneling of a D atom between the radicals in the experimental time scale. The possible recombination of the two radicals to butane is not observed at all. (II) $(C_2D_5I)_2 + h\nu \rightarrow CD_2{=}CD_2 + C_2D_6 + I_2$, which is a direct molecular process to give the same products as (I). The ethylene produced by both (I) and (II) tends to form complexes with C_2D_6 and with I_2. Prolonged irradiation induces the following secondary photolysis of the three primary photoproducts: $\bullet C_2D_5 + h\nu \rightarrow CD_2{=}CD_2 + \bullet D$, $DI + h\nu \rightarrow \bullet D + \bullet I$, and $I_2 + h\nu \rightarrow 2\bullet I$.

Introduction

Solid parahydrogen (p-H_2) matrix is a useful medium for the observation of photoinduced elementary processes. This is not only because the matrix is optically transparent but also because photofragments are separated enough by virtue of the extreme softness of the solid p-H_2, which is characteristic of a quantum solid.[1] The second feature cannot be overemphasized because photofragments in conventional rare gas matrixes suffer severe cage effects to leave no appreciable photolytic result in most cases.[2,3]

With the use of this advantageous feature of the p-H_2 matrix, we studied some time ago the photolysis of normal ethyl iodide, C_2H_5I,[4] to obtain further information on the ethyl radical, which had been studied by Pacansky et al. for a system of dipropionyl peroxide, $CH_3CH_2CO{-}O_2{-}COCH_2CH_3$, in rare gas matrixes.[5,6] The authors had to use the peroxide rather than ethyl iodide because the simpler ethyl iodide in rare gas matrixes is subjected to the recombination by the cage effect as has been confirmed by many authors.[2,3] The peroxide photolyzes into two ethyl radicals and two intervening carbon dioxide molecules as $H_5C_2\bullet + (CO_2)_2 + \bullet C_2H_5$. The carbon dioxide molecules function as a spacer, and the recombination of the radicals is prevented.

However, in Pacansky's system, there is a possibility that CO_2 perturbs the ethyl radical in one way or the other. Moreover, byproducts containing oxygen atoms may have been produced. In our previous system of ethyl iodide/p-H_2, the ethyl radical and the counterpart iodine atom can elude the recombination and the reaction mechanism is expected to be simpler than that of the peroxide system.

The major primary processes found in our previous work were as follows:[4] $C_2H_5I + h\nu \rightarrow \bullet C_2H_5 + \bullet I$ and $(C_2H_5I)_2 + h\nu \rightarrow 2\bullet C_2H_5 + I_2$ *and/or* $CH_2{=}CH_2 + C_2H_6 + I_2$. These primary processes were followed by secondary photolysis of the radical as $\bullet C_2H_5 + h\nu \rightarrow CH_2{=}CH_2 + \bullet H$.

The present work on the C_2D_5I system is intended to extend the previous study to obtain supporting evidence for the previous work and to find any isotopic effects anticipated. It is also desirable to find an answer to the unsolved problem of whether the above dimer photolysis proceeds concurrently or only one of the two reactions occurs.

As a result, the above ambiguity of the "and/or" is removed to conclude that the two reactions proceed in parallel; i.e., it is confirmed that under irradiation both the homolytic reaction, $(C_2D_5I)_2 + h\nu \rightarrow 2\bullet C_2D_5 + I_2$, and the disproportionation, $(C_2D_5I)_2 + h\nu \rightarrow CD_2{=}CD_2 + C_2D_6 + I_2$, take place parallelwise. The two near-lying radicals produced by the former reaction gradually disproportionate in the dark to the pair $CD_2{=}CD_2 + C_2D_6$ by a quantum tunneling of a deuterium between the two radicals. No deuterated butane is ever formed nor any H−D mixed products, which might be expected for the system of C_2D_5I embedded in the p-H_2 matrix.

As for the monomeric iodide, a molecular process of $C_2D_5I + h\nu \rightarrow CD_2{=}CD_2 + DI$ is found in addition to the familiar C−I bond dissociation of $C_2D_5I + h\nu \rightarrow \bullet C_2D_5 + \bullet I$. All the experimental findings are explained by a few key reactions quite consistently.

Experimental Section

The experimental procedure is similar to that of the previous work on the C_2H_5I system[4] except that perdeuterated ethyl iodide

† A preliminary result was reported at The Third International Conference on Cryocrystals and Quantum Crystals, July 28 to Aug 4, 2000, Szklarska Poreba, Poland.

* To whom correspondence should be addressed. E-mail:momose@kuchem.kyoto-u.ac.jp.

‡ Kyoto University.

§ Kanagawa Institute of Technology.

10.1021/jp004027g CCC: $20.00
Published on Web 03/10/2001

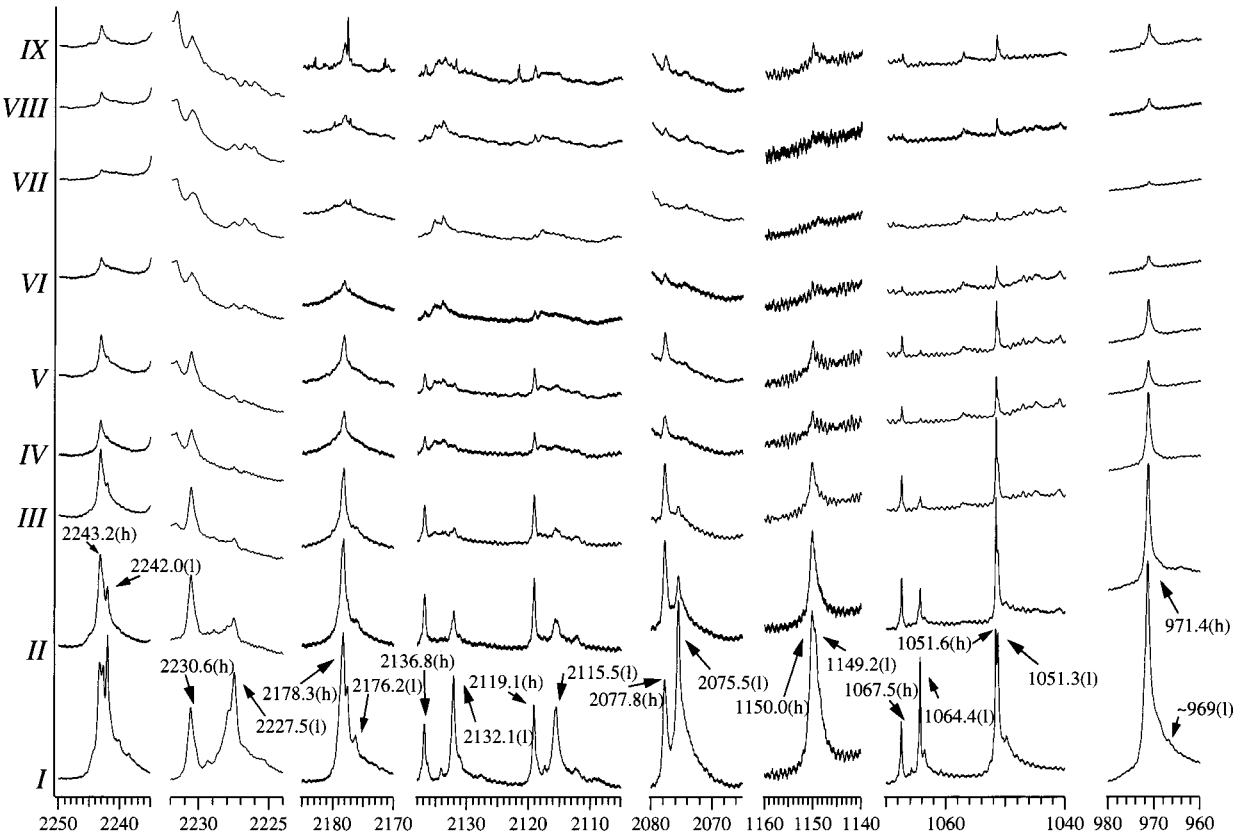

Figure 1. Infrared absorption spectra of C_2D_5I in solid *p*-H_2 at 4.4 K. Spectra I are for the sample before UV irradiation, II are the same as I after 60 min of irradiation, III are the same as I after 120 min of irradiation, IV are the same as I after 220 min of irradiation, V are the same as IV after a 12 h standing in the dark at 4.4 K, VI are the same as V after 100 min of irradiation. VII are the same as V after 380 min of irradiation, VIII are the same as VII after annealing at 5.5 K for 5 min and recooling to 4.4 K, IX are the same as VIII after annealing at 6.5 K for 5 min and recooling to 4.4 K.

from Euriso-top (isotopic purity of 99%) was used in place of C_2H_5I. Vaporized heavy iodide was mixed with gaseous *p*-H_2 (with ~0.001% orthohydrogen) to a pressure ratio of 1:10[4]. The mixed gas was introduced in about 1 h to a copper cell attached to the base of a cryostat at 8.2−8.3 K. The temperature was chosen to obtain a transparent sample, which was then carefully cooled to 4.4 K to avoid cracking. All the optical measurement was carried out at 4.4 K using a Bruker IFS-120HR FTIR spectrometer with a spectral resolution of 0.1 cm^{-1}. UV irradiation was performed using a 20 W low-pressure mercury lamp without optical filters. To examine the effect of thermal annealing, the sample either was kept at 4.4 K for 12 h in the dark or was warmed limitedly to 7.5 K for about 5 min at the end of each run of optical measurement. An MCT (mercury−cadmium−tellurium) detector was employed throughout the experiment.

Experimental Results

1. Ethyl Iodide. Figure 1 is reproduced from a typical run of experiment to demonstrate several spectral regions of C_2D_5I. Stage I corresponds to the spectra before UV irradiation. The subsequent spectra in stages II−IX are for the sample after continual irradiation and thermal annealing.

Figure 2 shows the relative absorbance A/A_0 of the iodide at various peak maxima, where A_0 is the initial absorbance of the peaks at stage I. As is seen from Figures 1 and 2, the absorption peaks due to the iodide are divided into two classes; class one appears at higher frequencies and decays relatively slowly upon photolysis but recovers partially upon warming to 6.5−7.5 K (peaks at 2243.2, 2230.6, 2178.3, 2136.8, 2119.1, 2077.8, 1150.0, 1067.5, 1051.6, and 971.4 cm^{-1}). The left-hand side panel of Figure 2 shows the temporal profile for this class of the iodide. Class two is red-shifted and disappears quickly with no recovery upon warming (peaks at 2242.0, 2227.5, 2176.2, 2132.1, 2115.5, 2075.5, 1149.2, 1064.4, 1051.3, and ~969 cm^{-1}). The right-hand side panel of Figure 2 is for this class. The separation between each pair of the two classes varies considerably; for example, the pair 2136.8 and 2132.1 cm^{-1} has a separation of ~5 cm^{-1}, while the pairs at about 1150, 1051, and 970 cm^{-1} are almost superposing. Hereafter, the iodides of classes one and two are conveniently called the high- and low-frequency iodides. The symbols "h" and "l" in Figure 1 stand for these two iodides.

From Figure 2 the half-life of A/A_0, i.e., the time at $A/A_0 = 1/2$, is roughly evaluated as 75 and 30 min for the high- and low-frequency iodides, respectively. A close examination of the temporal curves in Figure 2 reveals that the absorption of the high-frequency iodide is slightly enhanced when the sample irradiated for a total of 220 min was kept at 4.4 K for 12 h in the dark as is shown by the small vertical arrows in Figure 2a. The enhancement may also be visually recognized by careful comparison of the spectra at stages IV and V in Figure 1.

2. Ethylene. Ethylene was one of the major products in the previous study on the C_2H_5I system,[4] so also in the present system deuterated ethylene is expected to be major. According to the literature[7] the fundamentals of perdeuterated ethylene in the gas phase are as follows: 2345 cm^{-1} (ν_9, b_{2u}, CD a-stretch, strong), 2200.2 cm^{-1} (ν_{11}, b_{3u}, CD_2 a-stretch, strong), 1077.9 cm^{-1} (ν_{12}, b_{3u}, CD_2 scissors, strong), and 720.0 cm^{-1} (ν_7, b_{1u}, CD_2 wagging, very strong).

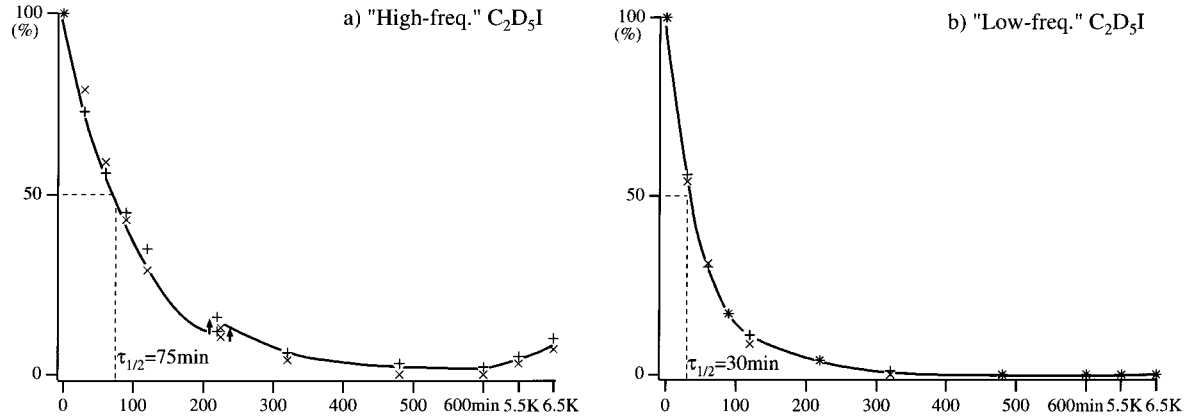

Figure 2. Temporal changes of the relative absorbance A/A_0 of the high-frequency ethyl iodide (panel a) and the low-frequency iodide (panel b) as a function of the irradiation time in minutes. The absorbance A_0 represents the initial absorbance at stage I. The representative peaks chosen are as follows: (a) (+) 971.4 cm^{-1}, (×) 1150.0 cm^{-1}; (b) (+) 1064.4 cm^{-1}, (×) 2075.5 cm^{-1}. The vertical arrows indicate a slight recovery of the intensity during the 12 h standing in the dark at 4.4 K. Both the arrowed + and × in Figure 2a are the plots for the same 220 min irradiation time, but they are slightly shifted horizontally for legibility. The two vertical dashes for 5.5 and 6.5 K in the abscissa are just to show the annealing temperatures, which are higher than the temperature of 4.4 K for the rest of the measurement.

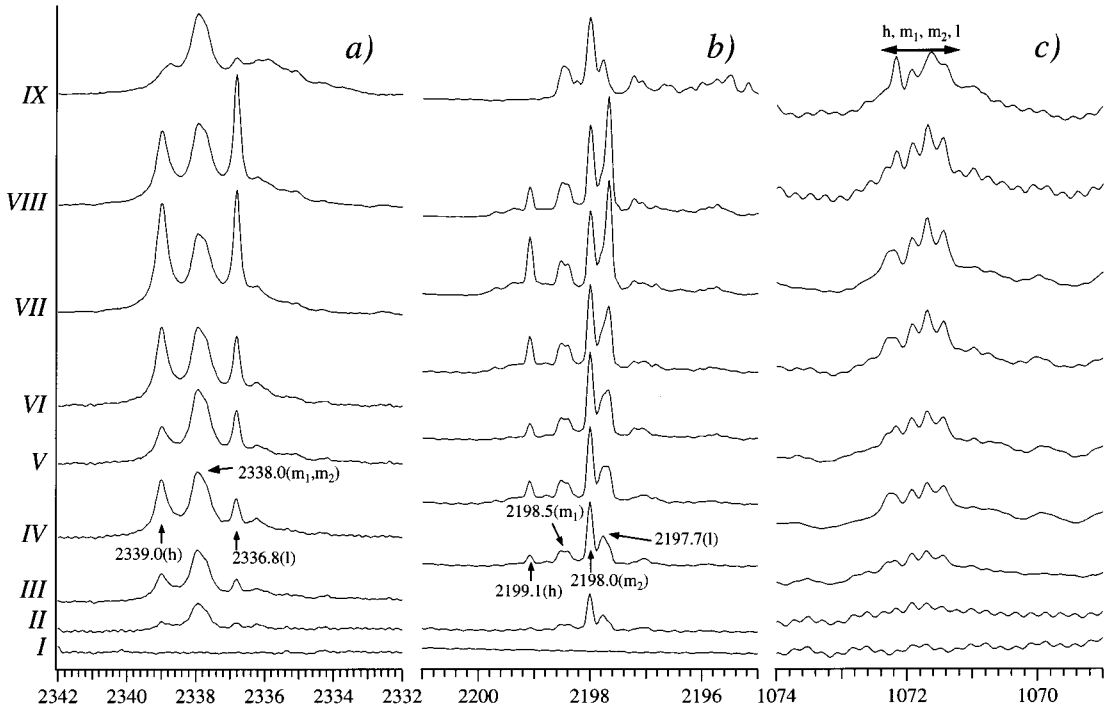

Figure 3. Infrared absorption spectra of $CD_2{=}CD_2$ in three spectral regions where the absorptions due to the deuterated ethylene appear. See the caption of Figure 1 also. (a) ν_9 region (2345 cm^{-1} in the gas). The peaks at 2339.0 cm^{-1} ("h"), 2338.0 cm^{-1} ("m_1"), 2338.0 cm^{-1} ("m_2"), and 2336.8 cm^{-1} ("l") are assigned to free ethylene, ethylene in the [$CD_2{=}CD_2{\cdots}C_2D_6$] complex, ethylene in the [$CD_2{=}CD_2{\cdots}DI$] complex, and ethylene in the [$CD_2{=}CD_2{\cdots}I_2$] complex, respectively. (b) ν_{11} region (2200.2 cm^{-1} in the gas). The peaks at 2199.1 cm^{-1} ("h"), 2198.0 cm^{-1} ("m_1"), and 2197.7 cm^{-1} ("l") are assigned the same as in (a). The peak at 2198.5 cm^{-1} marked with "m_1" is assigned to the ethylene in the [$CD_2{=}CD_2{\cdots}C_2D_6$] complex. (c) ν_{12} region (1077.9 cm^{-1} in the gas). The weak congested peaks at ~1073 to ~1070 cm^{-1} are regarded as the superposed absorptions of the "h", "m_1", "m_2", and "l" ethylenes.

In accordance with this literature information the sample after the irradiation exhibits the spectra assignable to ethylene as shown in Figure 3. The ν_7 band at 720.0 cm^{-1} in the literature is beyond the detection limit in the present work.

The apparently complicated spectral structures in Figure 3 suggest the coexistence of different components of ethylene. The occurrence of multiple components of ethylene is reminiscent of the occurrence of two components of ethylene in the previous work on the C_2H_5I system,[4] which were called the high- and low-frequency ethylenes. As in the previous work these components of ethylene will be associated with four kinds of complexes coupled with different partners (see subsections 5 and 6 of the Discussion). They are called conveniently the high, medium-1, medium-2, and low-frequency ethylenes and designated as "h", "m_1", "m_2", and "l", respectively. In Figure 3a the peaks at 2339.0 and 2336.8 cm^{-1} are well separated. They are assigned as the "h" and "l" ethylenes, respectively, but the peak at about 2338.0 cm^{-1} appearing between the "h" and "l" ethylenes seems to comprise two components denoted by "m_1" and "m_2". In Figure 3b the peaks at 2199.1, 2198.5, 2198.0, and 2197.7 cm^{-1} are assigned as the "h", "m_1", "m_2", and "l" ethylenes. Due to the severe overlap in Figure 3c, such resolution as in Figure 3a,b is not made, but it is likely that there are four components in this region also.

The assignment of the four different ethylenes in Figure 3a,b will be supported by the different temporal behavior of each

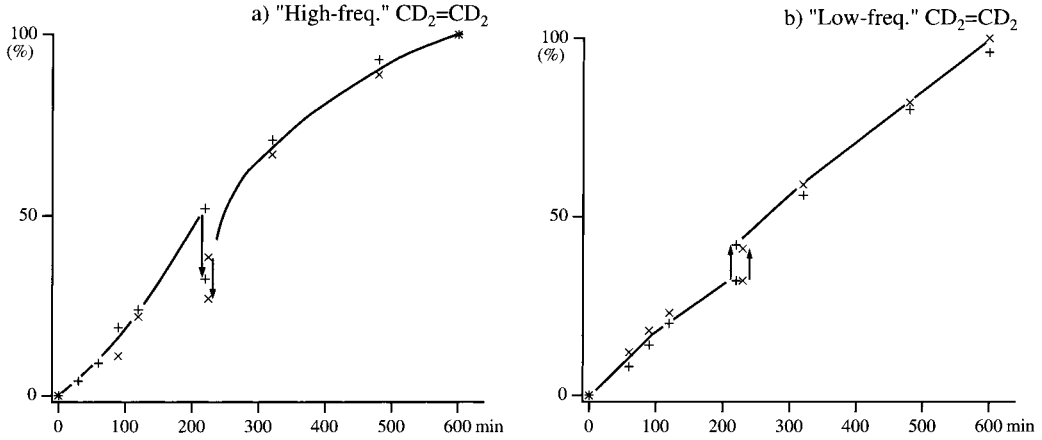

Figure 4. Temporal changes of the relative absorbance A/A_{max} of the high-frequency ethylene (panel a) and the low-frequency ethylene (panel b). The representative peaks chosen are as follows (see the caption of Figure 2 also): (a) (+) 2339.0 cm^{-1}, (×) 2199.1 cm^{-1}; (b) (+) 2336.8 cm^{-1}, (×) 2197.7 $cm-^{1}$.

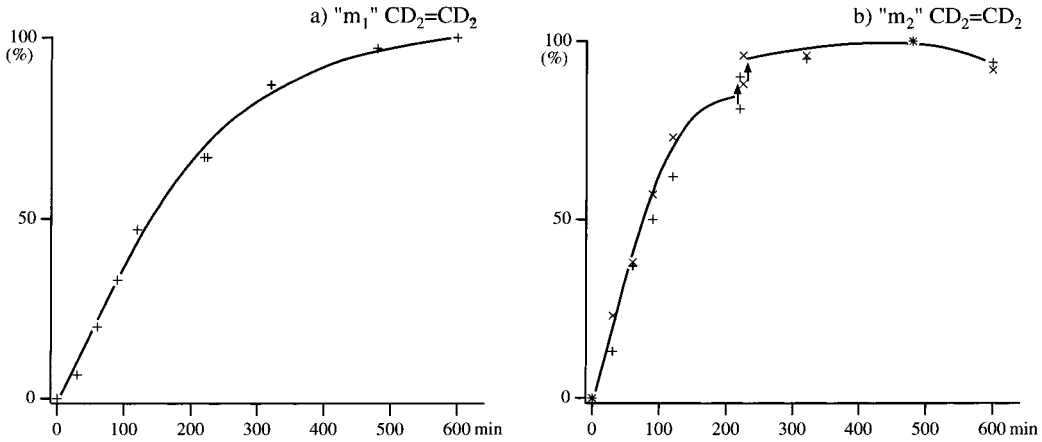

Figure 5. Temporal changes of the relative absorbance A/A_{max} of the two medium-frequency ethylene designated as "m_1" (panel a) and "m_2" (panel b). The representative peaks chosen are as follows (see the caption of Figure 2 also): (a) 2198.5 cm^{-1}; (b) (+) 2338.0 cm^{-1}, (×) 2198.0 cm^{-1}.

component as shown in Figures 4 and 5. Figures 4 and 5 demonstrate the temporal intensity profiles of the four ethylenes as a function of the time of irradiation. Figure 4a shows the relative absorbance A/A_{max} of the "h" ethylene at 2339.0 cm^{-1} ("h" in Figure 3a) and at 2199.1 cm^{-1} ("h" in Figure 3b), where A is the absorbance at various irradiation times and A_{max} is the maximum value of the absorbance. Figure 4b shows the change of the "l" ethylene at 2336.8 cm^{-1} ("l" in Figure 3a) and 2197.7 cm^{-1} ("l" in Figure 3b). Likewise, Figure 5a demonstrates the temporal profile of the relative absorbance of the medium-frequency ethylene at 2338.0 cm^{-1} ("m_1" in Figure 3a) and 2198.5 cm^{-1} ("m_1" in Figure 3b). Figure 5b is a similar plot for another medium-frequency ethylene at 2198.0 cm^{-1} ("m_2" in Figure 3b).

The profiles for the "h" and "l" ethylenes in Figure 4 differ remarkably from the profiles for the two medium-frequency ethylenes in Figure 5. The former two in Figure 4 increase rather monotonically with irradiation time except for the discrete changes at 220 min, whereas the latter two in Figure 5 indicate saturation to make the curves roughly upward convex. The difference will be consistently explained by referring to the profile of DI in Figure 8b (see subsections 5 and 6 of the Discussion). The vertical arrows in Figure 4 indicate the decrease of the "h" ethylene and the increase of the "l" ethylene during the dark period for 12 h at 4.4 K after the irradiation of a total of 220 min.

Similarly, the arrow in Figure 5b indicates a small increase of the "m_2 " ethylene during the same period (cf. Figure 3b for the spectrum). The implication of these apparently complex changes during the dark period is explained consistently in subsections 5 and 6 of the Discussion.

3. Ethane. By analogy with the previous work[4] ethane is expected to be another major product. The gas-phase frequencies of the fundamentals of C_2D_6 are as follows: 2236 cm^{-1} (ν_7, e_u, CD_3 d-stretch), 2087.4 cm^{-1} (ν_5, a_{2u}, CD_3 s-stretch), 1081.3 cm^{-1} (ν_8, e_u, CD_3 d-deformation), 1077.1 cm^{-1} (ν_6, a_{2u}, CD_3 s-deformation).[7]

In the spectral regions of all four cited fundamentals broad absorption bands appear as shown in Figure 6. The decaying absorptions of the ethyl iodide are also seen at 2230.6 and 2227.5 cm^{-1} in Figure 6a and at 2077.8 and 2075.5 cm^{-1} in Figure 6b (cf. Figure 1). These iodide peaks should be ignored here.

Figure 6a covers the spectral region of the ν_7 mode of gaseous ethane at 2236 cm^{-1} cited above. In this region two structured broad bands are observed at about 2235−2225 and 2225−2210 cm^{-1} as indicated by the two horizontal arrows. The appearance of two, rather than one, bands in the region of the single ν_7 mode is considered in subsection 4 of the Discussion. In Figure 6b a broad band is seen at about 2085−2077 cm^{-1} as indicated by the horizontal arrow, which corresponds well to the ν_5 mode of gaseous ethane at 2087.4 cm^{-1}. The band with the maximum at 1075.0 cm^{-1} in Figure 6c is comparable with the ν_8 mode of gaseous ethane at 1081.3 cm^{-1}. The structured absorption on the right-hand side of Figure 6c is the same as Figure 3c, but is reproduced because the absorption is regarded as accidentally

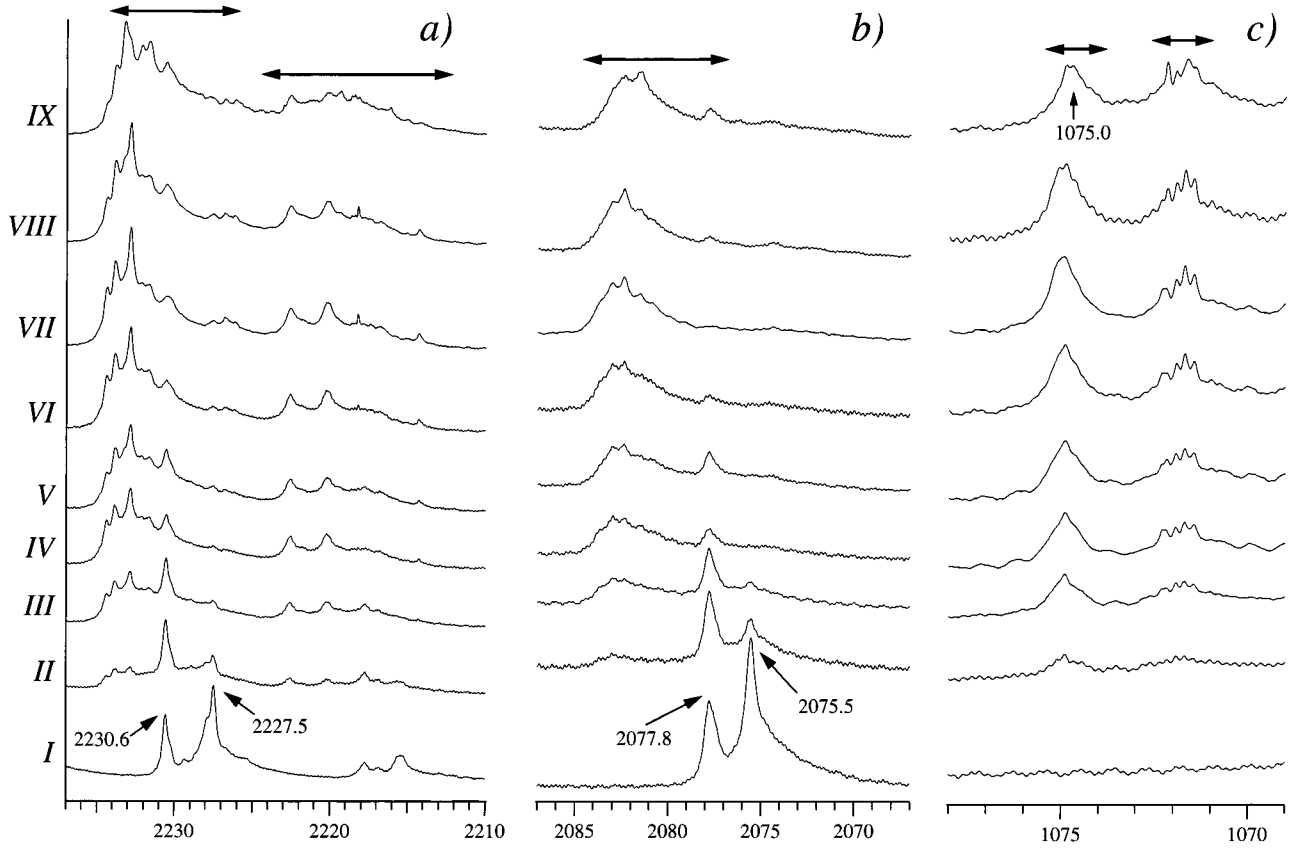

Figure 6. Infrared absorption spectra of ethane in three spectral regions where the absorptions due to ethane appear. See the caption of Figure 1 also for the spectra I−IX. (a) ν_7 region (2236 cm^{-1} in the gas). The broad bands at ∼2235 to ∼2225 cm^{-1} and at ∼2225 to ∼2210 cm^{-1} indicated by the horizontal bars are assigned to either the two split components of the ν_7 mode of e_u symmetry or to a pair of free ethane and ethane in the [C_2D_6···I_2] complex. The peaks at 2230.6 and 2227.5 cm^{-1} at the early stages of irradiation are due to the ethyl iodide (see Figure 1), which should be ignored here. (b) ν_5 region (2087.4 cm^{-1} in the gas). The broad band at ∼2085 to ∼2077 cm^{-1} indicated by the horizontal bar is assigned to the ν_5 mode of a_{2u} symmetry of ethane. The peaks at 2077.8 and 2075.5 cm^{-1} at the early stages of irradiation are due to the ethyl iodide (see Figure 1), which should be ignored here. (c) ν_8 and ν_6 regions (1081.3 and 1077.1 cm^{-1} in the gas). The broad band with the maximum at 1075.0 cm^{-1} indicated by the horizontal bar at the left is assigned to the ν_8 mode of ethane. The sharply structured peak at ∼1073 to ∼1070 cm^{-1} is associated with the ν_{12} mode of ethylene (see the caption for Figure 3c). It is assumed that these peaks are accidentally superimposed by the broad band of the ν_6 mode of ethane indicated by the horizontal bar at the right.

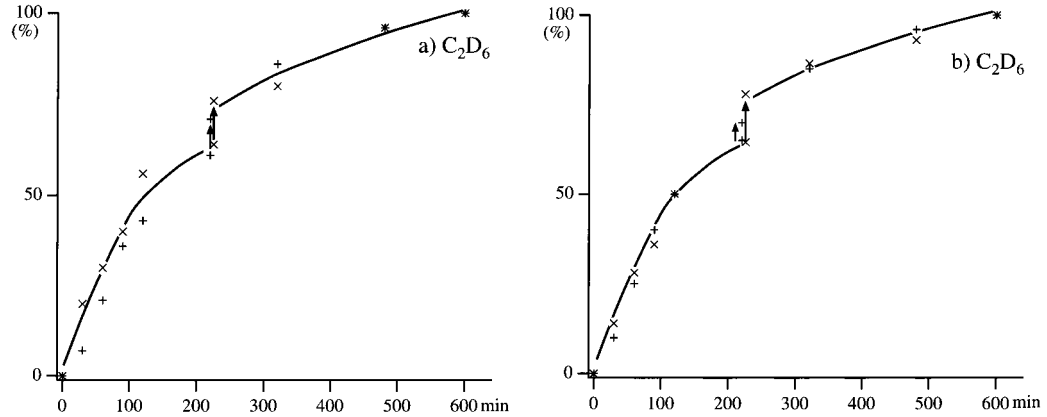

Figure 7. Temporal changes of the relative absorbance A/A_{max} of ethane. The plot was made at the following frequencies: (a) 2232.9 cm^{-1} (+), 2222.6 cm^{-1} (×); (b) 2082.4 cm^{-1} (+), 1075.0 cm^{-1} (×). These frequencies are chosen rather arbitrarily from the broad absorption bands shown in Figure 6. See the caption of Figure 2 also.

overlapped absorptions of ethane (the ν_6 region of gaseous ethane at 1077.1 cm^{-1}) and of ethylene (the ν_{12} region of gaseous ethylene at 1077.9 cm^{-1}). All the broad bands indicated by the five horizontal arrows in Figure 6 are considered as due to ethane because their temporal profiles are quite similar as shown in Figure 7.

Figure 7 shows the plot of the relative absorbance at the frequencies of 2232.9, 2222.6, 2082.4, and 1075.0 cm^{-1}, which are chosen rather arbitrarily from the broad absorption bands ascribed to ethane in Figure 6. To avoid the congestion of the plot, the figure is divided into two panels, but they superpose each other nicely. The vertical arrows in Figure 7 indicate the increase of ethane during the 12 h standing at 4.4 K.

4. DI and [CD_2═CD_2···•I] Complex. The peak at 1568.5 cm^{-1} in Figure 8a is attributed to DI because of its proximity to the literature frequency of ∼1530 cm^{-1} reported for the iodide

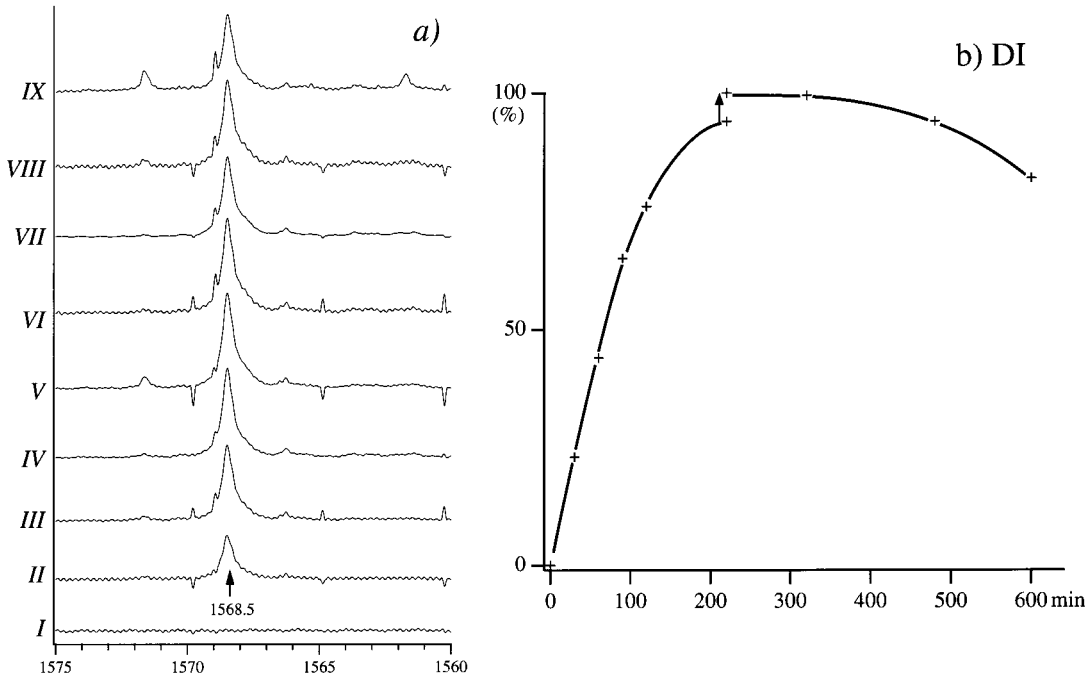

Figure 8. Infrared absorption spectra of DI (panel a) and its temporal behavior (panel b). The single peak at 1568.5 cm^{-1} in panel a is assigned to monomeric DI produced by reaction 6. Note the similarity between the profiles in Figures 5b and 8b. The slight decline of the curves in Figures 5b and 8b at later stages of irradiation is attributed to the secondary photolysis of DI, which destroys both DI itself and the [CD_2═CD_2┅DI] complex. See the captions of Figures 1 and 2 also for the spectra I−IX and the vertical arrow.

in low-temperature matrixes.[8] (In the previous work on the C_2H_5I system[4] the absorption of HI was overlooked. The absorption was later found at 2189.0 cm^{-1}, which is a significantly lower frequency than that reported in the literature, that is, at 2242 cm^{-1} in the gas phase assigned as R(0) and 2253−2237 cm^{-1} in Ar matrix.[8,9,10] Fortunately, however, this oversight of the HI absorption does not seriously affect the argument of the major reaction mechanism in the previous work.[4])

The single peak in Figure 8a indicates that the DI is isolated as a monomer because it is well-known that HI and DI are apt to form small clusters in matrixes and give rise to a number of peaks.

The temporal plot of the DI absorption at 1568.5 cm^{-1} is shown in Figure 8b, which bears resemblance to the plot for the "m_2" ethylene shown in Figure 5b. The resemblance suggests a parallel formation of DI and the "m_2" ethylene as is explored in subsection 5 of the Discussion.

The absorption peak at 2187.5 cm^{-1} in Figure 9a is close to the absorption of HI at 2189.0 cm^{-1} mentioned above. Therefore, one might consider that in the present system of C_2D_5I/*p*-H_2 the normal hydrogen iodide was produced by some mechanism. However, this possibility is denied on the basis that there are no H−D mixed products such as C_2D_5H which might be expected if HI were produced in the present system. The initially downward convex sigmoidal profile in Figure 9b for the 2187.5 cm^{-1} peak is consistently explicable in terms of a complex between a perdeuterated ethylene and an iodine atom, [CD_2═CD_2┅•I] (see subsection 7 of the Discussion). Thus, the proximity of this peak at 2187.5 cm^{-1} to the HI peak at 2189.0 cm^{-1} is regarded as accidental.

5. Ethyl Radical. The rest of the observed absorptions are collectively shown in Figure 10 at ∼2370 to ∼2360, ∼2358 to ∼2350, ∼2350 to ∼2343, 2092.2, 2060.7, 2050.0, and 1188.7 cm^{-1},which are indicated by the horizontal arrows. The temporal changes of some of the representative absorptions in Figure 10 are illustrated in Figure 11. Like Figure 6, the plot is divided into two panels to avoid congestion, but the profiles for the selected four frequencies are quite similar. The similarity of the temporal changes among the absorptions in Figure 10 strongly suggests that the absorbing species are common. In particular, all the absorptions decrease sensitively upon thermal annealing (compare the spectra in Figure 10 for stages VII at 4.4 K, VIII at 5.5 K, and IX at 6.5 K). The similar temporal behavior and the thermal instability indicate that the absorptions are due to the reactive ethyl radical.

Some of the frequencies of the peaks agree with the frequencies reported by Pacansky for the perdeuterated ethyl radical.[5,6] The partial disagreement with the literature is considered to be due to the fact that the work in the literature was carried out by photolyzing a rather complicated precursor of dipropionyl peroxide,[5,6] which may have produced byproducts other than the radical. The first very weak absorption at ∼2370 to ∼2360 cm^{-1} in Figure 10a may be due to the combination band of the strong absorption at 2050.0 cm^{-1} in Figure 10c (which corresponds to Pacansky's 2048 cm^{-1}) and the umbrella mode reported by Pacansky at 398 cm^{-1}.

The highest frequency of the perdeuterated ethyl radical reported by Pacansky is 2249 cm^{-1}.[5,6] However, in Figure 10a there are several bands at frequencies higher than Pacansky's value of 2249 cm^{-1}. Despite this difference from Pacansky's result, all the absorptions in Figure 10a are regarded as due to the radical because they correspond well to the absorptions due to the •C_2H_5 radical at 3122.8 cm^{-1} in the previous work[4] after the correction of the deuterium substitution effect on the frequency. Both the •C_2H_5 radical at 3122.8 cm^{-1} in the previous work[4] and the •C_2D_5 radical in Figure 10a of the present study appear at a little higher frequencies than the absorptions of the ν_9 mode of CH_2═CH_2 at 3103−3096 cm^{-1} in the previous work[4] and of CD_2═CD_2 at 2342−2325 cm^{-1} shown in Figure 3a.

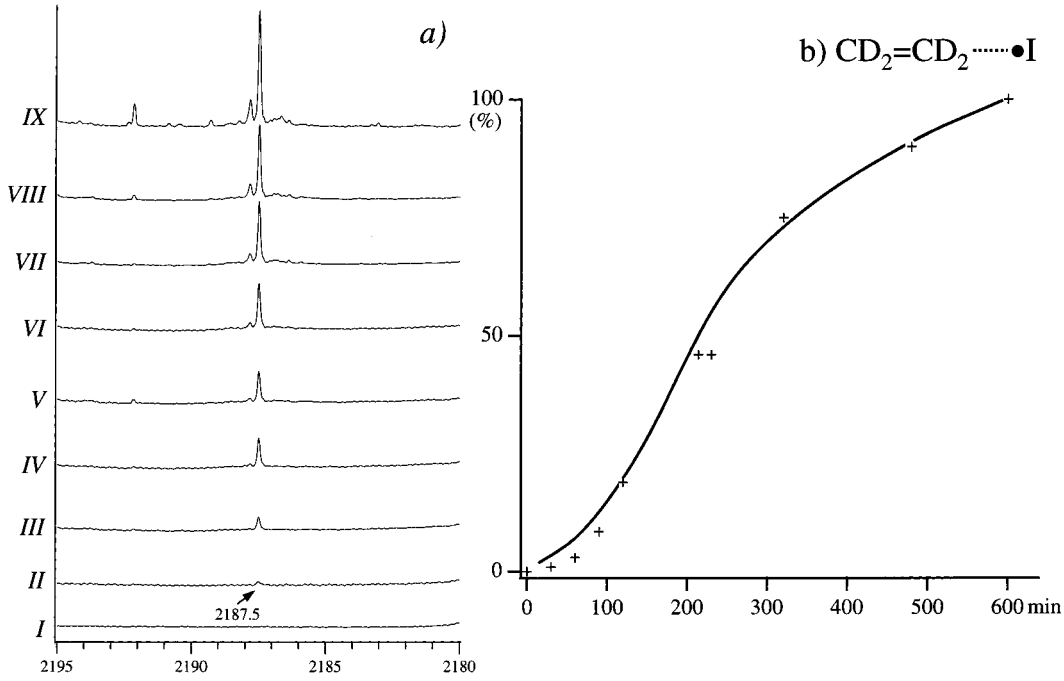

Figure 9. Infrared absorption spectra of the [CD_2═CD_2┅∞I] complex (panel a) and its temporal behavior (panel b). The peak at 2187.5 cm^{-1} in panel a is attributed to the [CD_2═CD_2┅•I] complex produced by reaction 1 followed by reaction 4. The sigmoidal curve for Figure 9b is reasonable because the coupled reactions 1 and 6 are a secondary photolytic reaction. The two plus signs at the irradiation time of 220 min are indistinguishably overlapped, but they are deliberately shifted for legibility in Figure 9b. See the caption of Figure 1 also for the spectra I−IX.

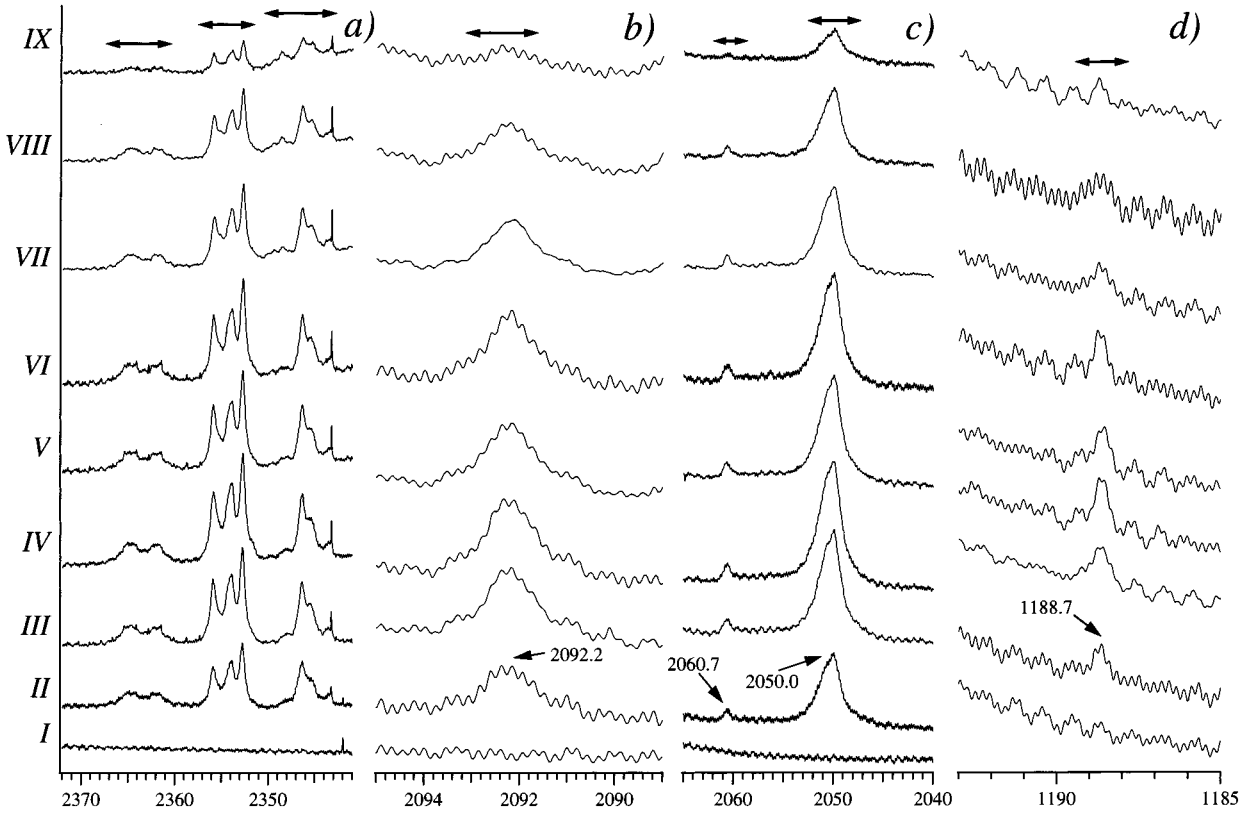

Figure 10. Infrared absorption spectra attributed to the perdeuterated ethyl radical. (a) It is presumed that at least three bands of the radical are seen at ∼2370 to ∼2360, ∼2358 to ∼2350, and ∼2350 to ∼2342 cm^{-1}. (b) The single peak at 2092.2 cm^{-1} is regarded as due to the radical. (c) The peaks at 2060.7 and 2050.0 cm^{-1} are assigned to the radical. (d) The single peak at 1188.7 cm^{-1} is attributed to the radical. See the caption of Figure 1 also for the spectra I−IX.

Discussion

For the convenience of readability of the following discussion, the symbols and the identification of various types of ethyl iodide and ethylene are first summarized in Table 1. For the same purpose, the overall reaction scheme to be concluded in the end is illustrated in Figure 12. The diagrams in Figure 12 are constructed on the basis of the facts that no H−D mixed hydrocarbons were observed and that the initial ethyl iodide exists in clearly different two forms, that is, monomeric and

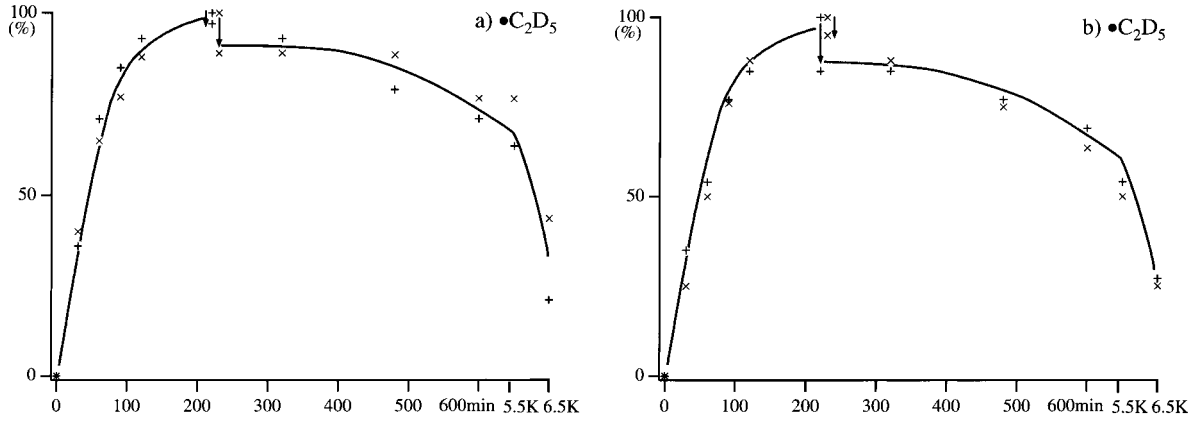

Figure 11. Temporal changes of the relative absorbance A/A_{max} of the perdeuterated ethyl radical. The representative peaks chosen are as follows: (a) (+) 2352.7 cm^{-1}, (×) 2346.4 cm^{-1}; (b) (+) 2050.0 cm^{-1}, (×) 2092.2 cm^{-1}. The vertical arrows indicate a decrease of the intensity during the 12 h standing in the dark at 4.4 K. See the caption of Figure 2 also.

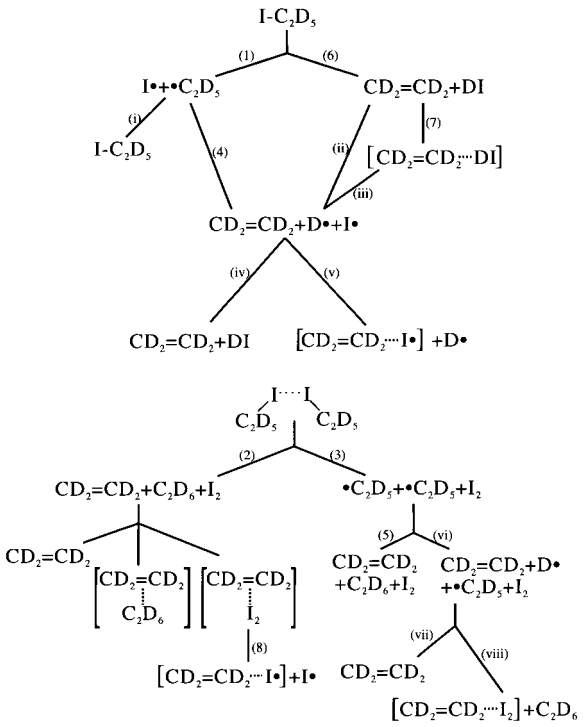

Figure 12. (Upper panel) Overall reactions initiated from the primary photolysis of monomeric ethyl iodide. The Roman numerals correspond to the steps explained in the text. The Arabic numbers represent the reaction numbering in the text. (Lower panel) Overall reactions initiated from the primary photolysis of dimeric ethyl iodide. The Roman numerals correspond to the steps explained in the text. The Arabic numbers represent the reaction numbering in the text.

TABLE 1: Symbols and Assignments of the Two Ethyl Iodides and the Four Ethylenes

ethyl iodide	high	C_2D_5I
	low	$(c_2D_5I)_2$
ethylene	high	free $CD_2{=}CD_2$
	medium-1	$CD_2{=}CD_2{\cdots}C_2D_6$
	medium-2	$CD_2{=}CD_2{\cdots}D_I$
	low	$CD_2{=}CD_2{\cdots}I_2$

dimeric, both of which are subjected to distinguishable photochemical processes.

In Figure 12, the Roman numerals will be used as the serial numbers for the various steps in the following discussion, while the Arabic numbers correspond to the numbering of the reactions in the text.

1. Monomeric and Dimeric Iodide. Besides the spectra at stage I in Figure 1, very weak absorptions are also observed at 2277, 2273, 2270, 2218, 2216, 2204, 2202, 2037, and 2019 cm^{-1}. Since the number of all these absorptions due to the ethyl iodide exceeds the number of the normal vibrational mode, the iodide must exist not only in monomers but also in clusters. On the basis of this assumption the photolysis of isolated monomeric iodides is considered first.

The partial recovery of the high-frequency ethyl iodide during the 12 h standing at 4.4 K and upon limited warming, shown in Figure 2a, indicates that the ethyl radical and the counterpart iodine atom produced from the isolated monomers are lying closely so that they are apt to be recombined to ethyl iodide. Thus, it is reasonable to assign the high-frequency iodide to the isolated monomeric iodide, which suffers the familiar photolysis in the following reaction:

$$C_2D_5I + h\nu \rightarrow \bullet C_2D_5 + \bullet I \qquad (1)$$

The photolysis and the recombination are indicated by reaction 1 and step i in the upper panel of Figure 12.

As for the low-frequency iodide, the previous work on the $C_2H_5I/p\text{-}H_2$ system strongly indicates that such an iodide is in dimeric form and is subjected to the following concerted one-photonic decompositions,[4] the location of which is shown in the lower panel of Figure 12:

$$(C_2D_5I)_2 + h\nu \rightarrow CD_2{=}CD_2 + C_2D_6 + I_2 \qquad (2)$$

and/or

$$(C_2D_5I)_2 + h\nu \rightarrow 2\bullet C_2D_5 + I_2 \qquad (3)$$

This type of one-photonic reaction proper to dimeric alkyl iodides has been studied in the gas phase using various experimental techniques.[11−14] A head-to-head configuration of R−I···I−R is commonly assumed for the dimer. The formation of both ethylene and ethane as shown in Figures 3−7 is in agreement with reaction 2.

It is commented that the dimeric unit considered here may not be necessarily an isolated dimer but the unit may be in trimers, tetramers, and other small clusters. The essential point is that the dimeric unit in such small clusters plays a role of an efficient antenna of single photons to initiate reactions 2 and/or 3. The clusters, however, cannot be so large as to be regarded as microcrystals of the iodide because preliminary test runs with higher concentrations of the iodide relative to the $p\text{-}H_2$ gave

structureless and significantly red-shifted bands assignable to the microcrystals.

2. Disproportionation Reaction. As in the case of the C_2H_5I/*p*-H_2 system,[4] no sign of the formation of butane is noticed, but only perdeuterated ethylene, ethane, and ethyl radical are detected. No H−D mixed products are ever detected as indicated by the absence of absorption due to C−H stretching modes in the spectral region of approximately 2850−2960 cm^{-1}. These results imply that the disproportionation of reaction 2 is preferred to the barrier-free dimerization to butane, which is intriguing.

The increase of the absorption of ethane (see the upward arrows in Figure 7) and the decrease of the absorption of ethyl radical (see the downward arrows in Figure 11) during the 12 h standing in the dark is understood in terms of a deuterium transfer from one radical to the other at 4.4 K via quantum tunneling on the time scale of the present experiment. Step 5 in the lower panel of Figure 12 indicates such a transfer.

3. Ethyl Radical. The above discussion presumes that the ethyl radical is produced not only by reaction 1 but also by reaction 3. If the radical were produced only by reaction 1, that is, if reaction 3 were absent, the rate of the growth of the radical should be similar to the rate of the slow decay of the high-frequency monomeric iodide, which is shown in Figure 2a. However, as shown in Figure 11, the initial growth of the radical is much faster, which implies that the radical is formed not only from monomeric ethyl iodide by reaction 1 but also from other sources too, which calls for reaction 3. Thus, the ambiguity implied by the notation of "and/or" in reaction 3 is ruled out definitely, and one can conclude that *both* reactions 2 and 3 take place.

It is well-known that the ethyl radical absorbs in the near-UV region covering the 253.7 nm radiation of the mercury lamp[15] and that the photoexcited radical splits the methyl C−D bond to yield ethylene[16] by reaction 4.

$$\bullet C_2D_5 + h\nu \rightarrow CD_2{=}CD_2 + \bullet D \qquad (4)$$

Therefore, when the radical by reaction 3, which accompanies an iodine molecule, is further photolyzed by reaction 4, it may yield both a free ethylene and an ethylene complexed with I_2 as [$CD_2{=}CD_2{\cdots}I_2$] (see steps vi−viii in Figure 12).

As shown in Figure 11, the intensity of the radical reaches the maximum after 220 min of irradiation. It decreases during the 12 h standing in the dark, while ethane in Figure 7 and the "l" ethylene in Figure 4b increase. In contrast, the "h" ethylene in Figure 4a decreases during the same dark period. These counterbalancing changes are understood by coupled reactions 3 and 5, provided that some of the ethylene in reaction 5 is slowly complexed with the iodine molecule in reaction 3:

$$\bullet C_2D_5 + \bullet C_2D_5 \rightarrow CD_2{=}CD_2 + C_2D_6 \qquad (5)$$

Figure 11 also shows a gradual decrease of the radical during the reirradiation period up to 600 min, which should reflect the depletion of the radical by reaction 4. The subsequent rapid decrease upon warming from 4.4 K by a few degrees may indicate that the deuterium transfer by reaction 5 is accelerated by the elevation of temperature.

4. Ethane. According to the reaction mechanism so far considered, ethane is produced by photolysis of reaction 2 and by the slow disproportionation via reaction 5. In both cases ethane is always accompanied by the near-lying iodine molecule produced by reactions 2 and 3, which may affect ethane either by complex formation ([$C_2D_6{\cdots}I_2$]) or by lifting the double degeneracy of the ν_7 and ν_8 modes of ethane of e_u symmetry. The appearance of the two broad bands at about 2235−2225 and 2225−2210 cm^{-1} in the ν_7 region of ethane in Figure 6a may be related to either possibility above. Whether or not the same argument is applicable to another e_u symmetry ν_8 mode of ethane in Figure 6c is unclear because of the accidental overlap of the absorption of the ν_6 (a_{2u}) mode of ethane and the ν_{12} mode of ethylene (see subsection 3 of the Experimental Results). However, the very similar upward convex curves at the four wavenumbers in Figure 7 strongly suggest that all four absorptions are due to ethane in common.

5. Medium-2-Frequency Ethylene and DI. It is assumed in Figures 3 that four different types of ethylene exist, which are designated as "h", "m_1", "m_2", and "l". It might seem arbitrary to assume various types of ethylene. However, the credence to the assignment of the four ethylenes will be given as follows.

The first clue to the assignment is to notice the similarity of the temporal change of the intensity of the "m_2" ethylene in Figure 5b to the change of DI shown in Figure 8b. The similarity can be understood if reaction 6 is assumed and some of the resulting ethylenes are complexed with the nascent DI by reaction 7 to give the absorption of the "m_2" ethylene.

$$C_2D_5I + h\nu \rightarrow CD_2{=}CD_2 + DI \qquad (6)$$

$$CD_2{=}CD_2 + DI \rightarrow [CD_2{=}CD_2{\cdots}DI] \qquad (7)$$

The heat deficiency of reaction 6, that is, $\Delta H_f^\circ(C_2D_4) + \Delta H_f^\circ(DI) - \Delta H_f^\circ(C_2D_5I)$ is tantamount to 52.4 + 26.5 − (−8.1) = 87.0 kJ/mol. This deficiency is well supplied by the 253.7 nm photon of the mercury lamp. Deuterium iodide might also be produced by the diffusive recombination between •D and •I atoms produced by such reactions as 1 and 4 and step iv in Figure 12. However, such a secondary recombination cannot be a major source of DI because the initial increase of DI during irradiation is very rapid as shown in Figure 8b.

Both Figures 5b and 8b show the leveling-off and the gradual decrease at later stages of irradiation. This is reasonable because DI, whether it is free as in reaction 6 or complexed with ethylene as in reaction 7, absorbs the near-UV photons competitively with ethyl iodide. These secondary photolyses are denoted by steps ii and iii in Figure 12, respectively. The UV absorption by DI destroys both the free DI and the DI moiety in the [$CD_2{=}CD_2{\cdots}DI$] complex. The small increase of the "m_2" ethylene during the 12 h standing at 4.4 K shown in Figure 5b is understood by assuming that reaction 7 proceeds gradually even at 4.4 K in the dark.

A closer comparison of Figures 5b and 8b, however, reveals two points to note: First, the decline of DI at the later stages in Figure 8b is slightly larger than the decrease of the [$CD_2{=}CD_2{\cdots}DI$] complex in Figure 5b. Second, DI itself also increases slightly during the dark standing as shown by the upward arrows in Figure 8b. The first point may indicate that the photosensitivity of the free DI is slightly larger than that of the DI moiety in the complex, even if the single peak at 1568.5 cm^{-1} in Figure 8a is common to the free DI and the DI moiety in the complex. As for the second point, it may be that the D atoms from the photolyzed DI may be recombined with •I as shown by step iv in Figure 12.

6. High-, Low-, and Medium-1-Frequency Ethylenes. Since reaction 2 yields three products, that is, $CD_2{=}CD_2$, C_2D_6, and I_2, some of the ethylenes produced by reaction 2 may be free and some others may be under the influence of ethane and iodine molecule. Excepting the "m_2" ethylene, which is already associated with the ethylene−DI complex in the preceding

subsection, there remain three ethylenes designated as "h", "m_1", and "l" in Figure 3. These three ethylenes are associated with the free ethylene and the complexes of [CD_2═CD_2···C_2D_6] and [CD_2═CD_2···I_2], respectively. The frequency of the "h" ethylene is the closest to the gas-phase value. The "l" ethylene is supposed to be most strongly affected by the iodine molecule, which has a sizable quadrupole moment.

As shown by the vertical arrows in Figure 4, the "h" ethylene diminishes and the "l" ethylene increases concomitantly during the 12 h standing at 4.4 K in the dark. The changes are reasonable because the three products of reaction 2 must be within a small space so that the ethylene may eventually find the iodine molecule to be complexed to give the "l" ethylene at the sacrifice of the "h" ethylene.

The free ethylene produced by reaction 4 after reaction 3 will add to the "h" ethylene originating from reaction 2. Likewise, the [CD_2═CD_2···I_2] complex produced by reaction 4 after reaction 3 should add to the "l" ethylene from reaction 2. Since these additional ethylenes via reaction 4 are the products of secondary photolysis of the radical, the additional contributions should have a sigmoidal (downward convex) growth curvature. The sum of the downward convex curves for these additional ethylenes and the upward convex curves for the ethylene via reaction 2 may compensate each other to give a relatively smooth curve (except for the discrete change at 220 min of irradiation) as shown Figure 4.

7. [CD_2═CD_2···•I] Complex. The spectrum in Figure 9a and the corresponding temporal change in Figure 9b remain to be explained. The sigmoidal growth of the intensity of the peak at 2187.5 cm^{-1} suggests that the absorption is due to a product of a secondary photolysis.

Photolysis of the ethyl radical originating from reaction 1 yields ethylene by reaction 4 (see the upper panel of Figure 12), but such an ethylene is accompanied by an iodine atom so that it is different from the ethylene formed by reaction 2 and by step vi after reaction 3, the latter two ethylenes being accompanied by an iodine molecule (see the lower panel of Figure 12). As stated in the preceding subsection, the overall growth curves for the latter ethylene, [CD_2═CD_2···I_2], consist of the upward and downward convex contributions to make the observed curves relatively smooth (Figure 4b). In contrast, there is no such compensating contribution for the ethylene produced by reaction 1 followed by reaction 4 so that only the sigmoidal curvature remains as observed in Figure 9b.

Figure 9b indicates that the intensity of the ethylene−iodine atom complex, [CD_2═CD_2···•I], does not change during the 12 h standing. This is understood if all the iodine atom by reaction 1 is complexed with the ethylene produced by the secondary photolysis of reaction 4 (see reaction 4 and step v in Figure 12). Figure 12 also shows that the same [CD_2═CD_2···•I] complex may be given by the routes of reactions 6 and 7 and steps iii and v.

However, if the [CD_2═CD_2···•I] complex were produced solely from monomeric ethyl iodides by the reactions discussed above, the growth of the complex would be limited by the exhaustion of the monomeric ethyl iodide, which occurs after about 300 min of irradiation according to Figure 2a. The continuing growth of the iodine atom complex beyond 300 min shown in Figure 9b can be accounted for by assuming that the [CD_2═CD_2···•I] complex may be produced from dimeric ethyl iodides also via the photolysis of the [CD_2═CD_2···I_2] complex by reaction 8.

$$I_2 + h\nu \rightarrow 2\bullet I \qquad (8)$$

The photolysis should transform the complex from [CD_2═CD_2···I_2] to [CD_2═CD_2···•I] (see reaction 8 in Figure 12). A similar transformation was considered in the previous work on the $C_2H_5I/p\text{-}H_2$ system.[4]

The peak position of the [CD_2═CD_2···•I] complex at 2187.5 cm^{-1} is even further red-shifted than that of the [CD_2═CD_2···I_2] complex at 2197.7 cm^{-1} (see Figure 3b for the low-frequency ethylene). A similar large red shift of the complex between ethylene and the atomic iodine was noted for the ν_7 mode of CH_2═CH_2 at about 950 cm^{-1} in the previous $C_2H_5I/p\text{-}H_2$ system.[4] The reason only the ν_{11} mode of ethylene exhibits such a remarkable red shift is unknown at the moment.

Conclusion

The present study has given strong credence to the mechanism of the major reactions of the previously studied $C_2H_5I/p\text{-}H_2$ system. As summarized in Figure 12, the absorption of one photon by both monomeric and dimeric ethyl iodides initiates parallel molecular and radical processes, that is, $C_2D_5I + h\nu \rightarrow CD_2$═$CD_2 + DI$ in competition with $\bullet C_2D_5 + \bullet I$ and $(C_2D_5I)_2 + h\nu \rightarrow CD_2$═$CD_2 + C_2D_6 + I_2$ along with $2\bullet C_2D_5 + I_2$. It is a new finding that the monomeric ethyl iodide decomposes by a direct molecular process to CD_2═CD_2 and DI.

It is surprising that complexation of ethylene to give [CD_2═CD_2···C_2D_6] ("m_1"), [CD_2═CD_2···DI] ("m_2"), [CD_2═CD_2···I_2] ("l"), and [CD_2═CD_2···•I] proceed even at 4.4 K and that the deuterium of the geminate radical pair transfers purely by quantum tunneling to result in the pair of ethylene and ethane. This unique disproportionation reaction supersedes the barrier-free recombination of the two radicals to butane.

Acknowledgment. This study was partially supported by a Grant-in-Aid for Scientific Research of the Ministry of Education, Science, Culture, and Sports of Japan.

References and Notes

(1) Momose, T.; Shida, T. *Bull. Chem. Soc. Jpn*. **1998**, *71*, 1
(2) Brus, L. E.; Bondybey, V. E. *J. Chem. Phys*. **1976**, *65*, 71
(3) Andrews, L.; Pimentel, G. C. *J. Chem. Phys.* **1967**, *47*, 3637
(4) Sogoshi, N.; Wakabayashi, T.; Momose, T.; Shida, T. *J. Phys. Chem. A* **1997**, *101*, 522.
(5) Pacansky, J.; Dupuis, M. *J. Am. Chem. Soc*. **1982**, *104*, 415.
(6) Pacansky, J.; Schrader, B. *J. Chem. Phys*. **1983**, *78*, 1033.
(7) Herzberg, G. *Molecular Spectra and Molecular Structure II. Infrared and Raman Spectra of Polyatomic Molecules*; Krieger Publishing Co.: Malabar, FL, 1991.
(8) Barnes, A. J.; Davies, J. B.; Hallam, H. E.; Howells, J. D. R. *J. Chem. Soc., Faraday Trans. 2* **1973**, 246.
(9) Fushitani, M.; Shida, T.; Momose, T.; Rasanen, M. *J. Phys. Chem.* **2000**, *101*, 3635.
(10) Engdahl, A.; Nelander, B. *J. Phys. Chem*. **1986**, *90*, 6118.
(11) Fan, Y. B.; Randall, K. L.; Donaldson, D. J. *J. Chem. Phys*. **1993**, *98*, 4700.
(12) Wang, P. G.; Zhang, Y. P.; Ruggles, C. J.; Ziegler, L. D. *J. Chem. Phys*. **1990**, *92*, 2806.
(13) Syage, J. A.; Steadman. *Chem. Phys. Lett*. **1990**, *166*, 159.
(14) Tanaka, Y.; Kawasaki, M.; Matsumi, Y. *Bull. Chem. Soc. Jpn*. **1998**, *71*, 2539.
(15) Wendt, H. R.; Hunziker, H. E. *J. Chem. Phys.* **1984**, *81*, 717.
(16) Brum, J. L.; Deshmukh, S.; Koplitz, B. *J. Chem. Phys*. **1991**, *95*, 2200.